

**CRYSTAL STRUCTURE OF ACPS/ACP COMPLEX,  
SOLUTION STRUCTURE OF *B. SUBTILIS* ACP, AND USES THEREOF**

This application claims the benefit of U.S. Provisional Application No. 60/202,466 filed May 8, 2000.

**Field of the Invention**

The present invention relates to the crystal structure of the ACPS/ACP complex, as well as the three-dimensional solution structure of *B. subtilis* ACP. These structures are critical for the design and selection of potent and selective agents which interact with ACPS and ACP, and particularly, the design of novel 5 antibiotics.

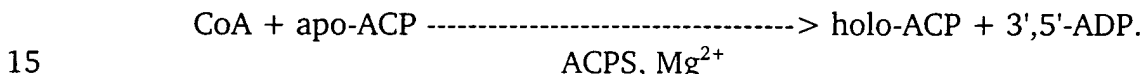
**Background of the Invention**

Acyl Carrier Proteins (ACPs) play important roles in a number of biosynthetic pathways that are dependent upon acyl group transfers [1]. They are 10 most often associated with the biosynthesis of fatty acids [2,3], but they are also utilized in the synthesis of polyketide antibiotics [4,5], non-ribosomal peptides [6,7], and of intermediates used in the synthesis of vitamins such as the protein-bound coenzymes, lipoic acid [8] and biotin [9]. The ACP in each of these 15 pathways is composed of 80-100 residues and is either an integrated domain in a larger multi-functional protein (Type I synthase complex) or is a structurally independent protein that is part of a non-aggregated multi-enzyme system (Type II synthase complex). Type I synthases are found in mammals, fungi and certain Mycobacteria while type II ACPs are utilized by plants and most bacteria. The *Escherichia coli* ACP for fatty acid synthesis has been over-expressed [10] and 20 purified [11,12], and the solution structure has been solved by NMR spectroscopy [13]. The fact that these proteins are essential for the maturation of the organism has led to their investigation as targets for the development of new anti-microbial agents [14-18].

Express Mail No. EL632297255US

ACPs require post-translational modification for activity. They are converted from an inactive apo-form to an active holo-form by the transfer of the 4'-phosphopantetheinyl (P-pant) moiety of coenzyme A to a conserved serine on the ACP. The  $\beta$ -hydroxy side chain of the serine residue serves as a nucleophilic group attacking the pyrophosphate linkage of CoA. Evidence now suggests [19] that each synthase that is dependent upon P-pant attachment for activation has its own partner enzyme responsible for this attachment.

The post-translational modification of the ACP subunit in the fatty acid synthase is performed by holo-[acyl carrier protein] synthase (hereinafter defined as “ACPS”; Enzyme Commission No. 2.7.8.7). The best characterized member of the ACPS family is the *E. coli* ACPS [20]. The enzyme produces holo-ACP by transferring the P-pant moiety to Ser-36 of the *E. coli* apo-ACP in a magnesium dependent reaction [20] as follows:



The over-expression and purification of the *E. coli* ACPS has been described [21] and this protein is classified as a member of a new enzyme superfamily, the phosphopantetheinyl transferases [19]. Based on the size of the proteins, the P-pant transferase superfamily can be roughly divided into two subgroups [22]. Enzymes responsible for modifying the peptidyl carrier protein subunits of non-ribosomal peptide synthetases are good examples for the first subgroup, which are usually ~ 230 amino acids in size. The structure of one of this subgroup enzymes, the surfactin synthetase activating enzyme Sfp, has been solved recently and it consists of a 2-fold intramolecular pseudosymmetry with the CoA binding site at the interface of the symmetrical fold [22]. ACPS and other enzymes transferring the P-pant group onto domains of the fatty acid synthases are usually smaller, about ~120 residues, and belong to the second subgroup of the P-pant transferase superfamily. The sequence homology between these two subgroups is

rather low, about 12-22% between *E. coli* ACPS and *B. subtilis* Sfp, for example, although both have been shown to possess P-pant transferase activity. Alignment [19] of some of these proteins show that two regions, residues 5-13 and 54-65 (*E. coli* ACPS numbering), are highly conserved with five of the residues in these  
5 regions identical.

While numerous members of the phosphopantetheinyl transferase superfamily have been identified and sequenced, until the present invention, the crystal structure of ACPS complexed with halo-ACP, and the three dimensional structure of the ACPS/ACP active site has not been determined. Further, prior to  
10 the present invention, the solution structure of *B. subtilis* ACP had not been determined.

#### Summary of the Invention

The present invention relates to a crystallized complex comprising an acyl carrier protein synthase (ACPS) and an acyl carrier protein (ACP) (hereinafter  
15 referred to as "ACPS-ACP complex"). The invention is further directed to the three dimensional structure of the ACPS-ACP complex, as determined using crystallographic analysis (with or without sedimentation analysis) of the ACPS-ACP complex. Particularly, the invention is directed to the three dimensional structure  
20 of the ACP binding site present in ACPS and other ACPS-like P-pant transferases, alone, and as complexed with ACP or other agents that interact with the ACP binding site of said transferases. In addition, the invention is directed to the ACPS binding site on ACP. Identification of the three dimensional structure of the ACP binding site on ACPS and the ACPS binding site on ACP will be valuable for the  
25 design of antibiotics and other agents that interfere with P-pant attachment, thereby preventing activation of corresponding carrier proteins.

The invention additionally provides a method for identifying an agent that interacts with any active site of an ACPS-ACP complex, comprising the steps of determining a putative active site of an ACPS-ACP complex from a three

dimensional model of the ACPS-ACP complex, and performing various computer fitting analyses to identify an agent which interacts with the putative active site. Again, such agents may act as inhibitors or activators of ACPS-ACP complex activity, as determined by obtaining the identified agent, contacting the same with

5 ACPS-ACP complex, and measuring the agent's effect on ACPS-ACP complex activity.

In addition, the invention provides a solution comprising *B. subtilis* ACP having a three dimensional structure defined by the structural coordinates of Figure 5,  $\pm$  a root mean square deviation from the backbone atoms of said amino acids of not more than 1.5 $\text{\AA}$ . Also provided by the invention is any active site of *B. subtilis* ACP that is defined by the structural coordinates of Figure 5,  $\pm$  a root mean square deviation from the backbone atoms of said amino acids of not more than 1.5 $\text{\AA}$ . Further, the present invention provides a method for identifying an agent that interacts with any active site of *B. subtilis* ACP, comprising the steps of

10 determining a putative active site of ACP from a three dimensional model of the ACP, and performing various computer fitting analyses to identify an agent which interacts with the putative active site. Again, such agents may act as inhibitors or activators of ACP activity, as determined by obtaining the identified agent,

15 contacting the same with ACP, and measuring the agent's effect on ACP activity.

20 Yet another aspect of the present invention is a method for identifying an activator or inhibitor of any molecule or molecular complex which comprises an ACP binding site, including any member of the ACPS-like P-pant transferases, comprising the steps of generating a three dimensional model of said molecule or molecular complex using the relative structural coordinates according

25 to Figure 3 of residues ARG14, MET18, ARG21, GLN22, ARG24, PHE25, ARG28, PHE54, GLU58, ILE68, GLY69, ALA70, SER73 and PHE74 from a first monomer of ACPS, and residue ARG45 from a second monomer of ACPS, or additionally, of residues ASP8, ILE9, THR10, GLU11, LEU12, ILE15, ALA16, SER17, ALA19, GLY20, ALA23, ALA26, GLU27, ILE29, ALA51, LYS57, SER61, LYS62, THR66,

GLY67, GLN71, LEU72, GLN75, ASP76, ILE77 and LYS93 from the first monomer of ACPS and residues LEU41, SER42, LYS44, GLU48, GLN83, ASN84, HIS105, THR106 and ALA107 from the second monomer of ACPS, in each case  $\pm$  a root mean square deviation from the backbone atoms of said amino acids of not more than 1.5 $\text{\AA}$ , and then selecting or designing a candidate activator or inhibitor that interacts with said molecule or molecular complex using computer fitting analyses of interactions between the three dimensional model of the molecule or molecular complex and the candidate activator or inhibitor. The effect of the candidate activator or inhibitor may be evaluated by obtaining the candidate activator or inhibitor, contacting the same with the molecule or molecular complex, and measuring the effect of the candidate activator or inhibitor on molecular or molecular complex activity.

In addition, the present invention provides a method for identifying an activator or inhibitor of any molecule or molecular complex which comprises an ACPS binding site, comprising the steps of generating a three dimensional model of said molecule or molecular complex comprising an ACPS binding site using the relative structural coordinates according to Figure 3 or 5 of residues ARG14, LYS29, ASP35, SER36, LEU37, ASP38, VAL40, GLU41, VAL43, MET44, GLU47, ASP48, ILE54, SER55, ASP56, GLU57 and GLU60, or additionally, of residues ASP13, LEU15, PHE28, GLU30, ASP31, LEU32, GLY33, ALA34, VAL39, LEU42, GLU45, LEU46, GLU49, MET52, GLU53, ASP58, ALA59, and LYS61, in each case  $\pm$  a root mean square deviation from the backbone atoms of said amino acids of not more than 1.5 $\text{\AA}$ , and then selecting or designing a candidate activator or inhibitor that interacts with said molecule or molecular complex using computer fitting analyses of interactions between the three dimensional model of the molecule or molecular complex and the candidate activator or inhibitor. The effect of the candidate activator or inhibitor may be evaluated by obtaining the candidate activator or inhibitor, contacting the same with the molecule or molecular complex, and measuring the effect of the candidate activator or inhibitor on molecular or

molecular complex activity. Also provided by the present invention are the activators or inhibitors selected or designed using the above-noted methods.

Still further, the present invention is directed to a method of determining the three dimensional structure of a molecule or molecular complex

- 5 whose structure is unknown, comprising the steps of first obtaining crystals of the molecule or molecular complex whose structure is unknown, and then generating X-ray diffraction data from the crystallized molecule or molecular complex. The X-ray diffraction data from the molecule or molecular complex is compared with the known three dimensional structures determined from the ACPS-ACP crystals of the  
10 present invention, and molecular replacement analysis is used to conform the known three dimensional structures to the X-ray diffraction data from the crystallized molecule or molecular complex.

In addition, the present invention provides the ACP active site of an ACPS-like P-pant transferase, including, but not limited to, an ACPS, comprising

- 15 the structural coordinates according to Figure 3 of residues ARG14, MET18, ARG21, GLN22, ARG24, PHE25, ARG28, PHE54, GLU58, ILE68, GLY69, ALA70, SER73 and PHE74 from a first monomer of ACPS, and residue ARG45 from a second monomer of ACPS, in each case  $\pm$  a root mean square deviation from the backbone atoms of said amino acids of not more than 1.5 $\text{\AA}$ . In another  
20 embodiment, the active site may include, in addition to the structural coordinates above, the relative the structural coordinates according to Figure 3 of residues ASP8, ILE9, THR10, GLU11, LEU12, ILE15, ALA16, SER17, ALA19, GLY20, ALA23, ALA26, GLU27, ILE29, ALA51, LYS57, SER61, LYS62, THR66, GLY67, GLN71, LEU72, GLN75, ASP76. ILE77 and LYS93 from one monomer of ACPS and residues  
25 LEU41, SER42, LYS44, GLU48, GLN83, ASN84, HIS105, THR106 and ALA107 from a second monomer of ACPS, in each case  $\pm$  a root mean square deviation from the backbone atoms of said amino acids of not more than 1.5 $\text{\AA}$ .

Finally, the present invention provides the ACPS active site of ACP, comprising the structural coordinates according to Figure 3 or 5 of residues ARG14,

LYS29, ASP35, SER36, LEU37, ASP38, VAL40, GLU41, VAL43, MET44, GLU47, ASP48, ILE54, SER55, ASP56, GLU57 and GLU60, in each case  $\pm$  a root mean square deviation from the backbone atoms of said amino acids of not more than 1.5 $\text{\AA}$ . In another embodiment, the active site may include, in addition to the

- 5 structural coordinates above, the relative structural coordinates according to Figure 3 or 5 of residues ASP13, LEU15, PHE28, GLU30, ASP31, LEU32, GLY33, ALA34, VAL39, LEU42, GLU45, LEU46, GLU49, MET52, GLU53, ASP58, ALA59, and LYS61,  $\pm$  a root mean square deviation from the backbone atoms of said amino acids of not more than 1.5 $\text{\AA}$ .

10

#### Brief Description of the Figures

Figure 1 depicts the amino acid sequences for the forms of ACP and ACPS used in the growth of ACP/ACPS complex crystals.

Figure 2 illustrates the alignment of amino acid sequences for twelve members of the ACPS family, including the consensus sequence.

15

Figure 3 provides the atomic structural coordinates for ACPS and ACP as derived by X-ray diffraction of an ACPS-ACP crystal. "Atom type" refers to the atom whose coordinates are being measured. "Residue" refers to the type of residue of which each measured atom is a part - i.e., amino acid, cofactor, ligand or solvent. The "x, y and z" coordinates indicate the Cartesian coordinates of each 20 measured atom's location in the unit cell ( $\text{\AA}$ ). "Occ" indicates the occupancy factor. "B" indicates the "B-value", which is a measure of how mobile the atom is in the atomic structure ( $\text{\AA}^2$ ). "MOL" indicates the segment identification used to uniquely identify each molecule. Under "MOL", "A1", "B1" and "C1" refers to each molecule of ACPS, "AP1", "AP2" and "AP3" refers to each molecule of ACP, and "W" 25 refers to water molecules.

Figure 4 represents the sequence alignment of *B. subtilis* ACP, *E. coli* ACP and *Streptomyces coelicolor* A3(2) ACP.

Figure 5 provides the atomic structural coordinates for the restrained minimized mean structure of *B. subtilis* ACP as derived by NMR spectroscopy.

“Atom type” refers to the atom whose coordinates are being measured. “Residue” refers to the type of residue of which each measured atom is a part - i.e., amino

- 5 acid, cofactor, ligand or solvent. The “x, y and z” coordinates indicate the Cartesian coordinates of each measured atom’s location (Å). The last column indicates the temperature factor field, representing the rms deviation of the 22 individual NMR structures about the restrained minimized mean structure. All non-protein atoms are listed as HETATM instead of atoms using PDB conventions.

10

#### Detailed Description of the Invention

As used herein, the following terms and phrases shall have the meanings set forth below:

- “ACPS” includes acyl carrier protein synthases as well as “ACPS-like”  
15 P-pant transferases. Acyl carrier protein synthases produce a holo-fatty acid synthase ACP by transferring the P-pant moiety to Ser-36 (or equivalent Serine) of an apo-fatty acid synthase ACP in a magnesium dependent reaction. “ACPS-like” P-pant transferases are those enzymes having P-pant transferase activity (i.e., that transfer the 4'-phosphopantetheinyl moiety of CoA to a conserved serine on the  
20 corresponding target molecule) which form homodimers and activate the ACP domains or subunits of fatty acid synthases, polyketide synthases or other enzymes.

- As used herein, “ACP” is the carrier of fatty acids during fatty acid biosynthesis, is responsible for acyl group activation and includes a 4'phosphopantetheine (4'-PP) prosthetic group in which the 4'-PP moiety is  
25 attached through a phosphodiester linkage to a specific conserved serine residue. “ACP” also includes an active (holo) and inactive (apo) form where activation of ACP is mediated by Holo-acyl carier protein synthase (ACPS), and is preferably the active (holo) form.

Unless otherwise indicated, "protein" shall include a protein, protein domain, polypeptide or peptide.

"Structural coordinates" are the Cartesian coordinates corresponding to an atom's spatial relationship to other atoms in a molecule or molecular

- 5 complex. Structural coordinates may be obtained using x-ray crystallography techniques or NMR techniques, or may be derived using molecular replacement analysis or homology modeling. Various software programs allow for the graphical representation of a set of structural coordinates to obtain a three dimensional representation of a molecule or molecular complex. The structural coordinates of
- 10 the present invention may be modified from the original sets provided in Figures 3 or 5 by mathematical manipulation, such as by inversion or integer additions or subtractions. As such, it is recognized that the structural coordinates of the present invention are relative, and are in no way specifically limited by the actual x, y, z coordinates of Figures 3 and 5.

- 15 An "agent" shall include a protein, polypeptide, peptide, nucleic acid, including DNA or RNA, molecule, compound, antibiotic or drug.

"Root mean square deviation" is the square root of the arithmetic mean of the squares of the deviations from the mean, and is a way of expressing deviation or variation from the structural coordinates of ACPS and ACP described

- 20 herein. The present invention includes all embodiments comprising conservative substitutions of the note amino acid residues resulting in same structural coordinates within the stated root mean square deviation.

It will be obvious to the skilled practitioner that the numbering of the amino acid residues in the various isoforms of ACPS, other ACPS-like P-pant

- 25 transferases and ACP may be different than that set forth herein or may contain certain conservative amino acid substitutions that yield the same three dimensional structures as those defined in Figures 3 and 5. Corresponding amino acids and conservative substitutions in other isoforms or analogues are easily identified by

visual inspection of the relevant amino acid sequences or by using commercially available homology software programs (e.g., MODELLAR, MSI, San Diego, CA).

“Conservative substitutions” are those amino acid substitutions which are functionally equivalent to the substituted amino acid residue, either by way of

- 5 having similar polarity, steric arrangement, or by belonging to the same class as the substituted residue (e.g., hydrophobic, acidic or basic) and includes substitutions having an inconsequential effect on the three dimensional structure of the ACPS-ACP complex, and the solution structure of *B. subtilis* ACP, with respect to the use of said structures for the identification and design of agents which interact with
- 10 ACPS and ACP, for molecular replacement analyses and/or for homology modeling.

As used herein, an “active site” refers to a region of a molecule or molecular complex that, as a result of its shape and charge potential, favorably interacts or associates with another agent (including, without limitation, a protein, polypeptide, peptide, nucleic acid, including DNA or RNA, molecule, compound,

- 15 antibiotic or drug) via various covalent and/or non-covalent binding forces.

As such, the active site of the ACPS-ACP complex may include both the actual site of ACP binding with ACPS, as well as accessory binding sites adjacent or proximal to the actual site of ACP binding that nonetheless may affect ACPS, ACPS-ACP or ACP activity upon interaction or association with a particular

- 20 agent, either by direct interference with the actual site of ACP binding or by indirectly affecting the steric conformation or charge potential of the ACPS molecule and thereby preventing or reducing ACP binding to ACPS at the actual site of ACP binding. As used herein, an active site of ACPS-ACP also includes ACPS or ACPS analog residues which exhibit observable NMR perturbations in the
- 25 presence of a binding ligand, such as ACP. While such residues exhibiting observable NMR perturbations may not necessarily be in direct contact with or immediately proximate to ligand binding residues, they may be critical to ACPS residues for rational drug design protocols.

- The active site of ACP includes a region of ACP that, as a result of its shape and charge potential, favorably interacts or associates with another agent (including, without limitation, a protein, polypeptide, peptide, nucleic acid, including DNA or RNA, molecule, compound, antibiotic or drug) via various
- 5 covalent and/or non-covalent binding forces. Preferably, the active site on ACP is the site of interaction with ACPS.

The present invention is directed to a crystallized ACPS-ACP complex that effectively diffracts X-rays for the determination of the structural coordinates of the ACPS-ACP complex. As used herein, the proteins used in the ACPS-ACP

10 crystal complex of the present invention includes any ACPS or ACP protein (i.e., as used herein, any protein, polypeptide or peptide), isolated from any source (including, but not limited to, a protein isolated from *Aquifex*, *Chlamydophila*, *Helicobacter*, *Staphylococcus*, *Thermotoga*, *Escherichia*, *Rickettsia*, *Streptomyces*, *Treponema*, *Bacillus*, *Bradyrhizobium*, and *Mycobacterium*). In a preferred

15 embodiment of the invention, ACPS and ACP are both cloned and isolated from *B. subtilis*, and overexpressed in a commercially available *E. coli* system.

The ACPS protein in the ACPS/ACP complex includes ACPS as well as proteins having ACPS-like P-pant transferase activity, including the consensus sequence shown in Figure 2. More preferably, the ACPS protein or proteins having

20 ACPS-like P-pant transferase activity, comprises the relative structural coordinates according to Figure 3 for the residues ARG14, MET18, ARG21, GLN22, ARG24, PHE25, ARG28, ARG45, PHE54, GLU58, ILE68, GLY69, ALA70, SER73 and PHE74, or conservative substitutions thereof, and additionally, the residues ASP8, ILE9, THR10, GLU11, LEU12, ILE15, ALA16, SER17, ALA19, GLY20, ALA23, ALA26,

25 GLU27, ILE29, LEU41, SER42, ALA44, GLU48, ALA51, LYS57, SER61, LYS62, THR66, GLY67, GLN71, LEU72, GLN75, ASP76, ILE77, GLN83, ASN84, LYS93, HIS105, THR106 and ALA107, or conservative substitutions thereof. More particularly, the ACPS protein or proteins having ACPS-like P-pant transferase activity include an ACP binding site defined using the relative structural

coordinates according to Figure 3 of residues ARG14, MET18, ARG21, GLN22, ARG24, PHE25, ARG28, PHE54, GLU58, ILE68, GLY69, ALA70, SER73 and PHE74 from a first monomer of ACPS, and residue ARG45 from a second monomer of ACPS, or additionally including the relative structural coordinates of residues ASP8,

5 ILE9, THR10, GLU11, LEU12, ILE15, ALA16, SER17, ALA19, GLY20, ALA23, ALA26, GLU27, ILE29, ALA51, LYS57, SER61, LYS62, THR66, GLY67, GLN71, LEU72, GLN75, ASP76, ILE77 and LYS93 from the first monomer of ACPS and residues LEU 41, SER42, ALA44, GLU48, GLN83, ASN84, HIS105, THR106 and ALA107 from the second monomer of ACPS. In each case, the  $\pm$  a root mean

10 square deviation from the backbone atoms of the amino acids is not more than 1.5 $\text{\AA}$ , more preferably not more than 1.0 $\text{\AA}$ , and most preferably, not more than 0.5 $\text{\AA}$ .

The ACP protein in the ACPS/ACP complex includes ACP and proteins having ACP activity, and preferably comprises the relative structural coordinates

15 accordingly to Figure 3 or 5 for the residues ARG14, LYS29, ASP35, SER36, LEU37, ASP38, VAL40, GLU41, VAL43, MET44, GLU47, ASP48, ILE54, SER55, ASP56, GLU57 and GLU60, or conservative substitutions thereof, and additionally, the residues ASP13, LEU15, PHE28, LYS29, GLU30, ASP31, LEU32, GLY33, ALA34, ASP35, SER36, LEU37, ASP38, VAL39, LEU42, GLU45, LEU46, GLU49, MET52,

20 GLU53, ASP58, ALA59 and LYS61, or conservative substitutions thereof, in each case  $\pm$  a root mean square deviation from the backbone atoms of said amino acids of not more than 1.5 $\text{\AA}$ , or more preferably not more than 1.0 $\text{\AA}$ , or most preferably, not more than 0.5 $\text{\AA}$ .

The crystals of the present invention may take a wide variety of

25 forms, all of which are included in the present invention. However, in a preferred embodiment of the present invention, the ACPS-ACP crystallized complex is characterized as being in rod-shape form with space group C222<sub>1</sub>, and having unit cell parameters of  $a=78.46 \text{ \AA}$ ,  $b=122.03 \text{ \AA}$  and  $c=136.77 \text{ \AA}$ , and consists of three molecules of ACPS and three molecules of ACP in an asymmetric unit.

Once a crystal or crystal complex of the present invention is grown, X-ray diffraction data can be collected by a variety of means in order to obtain the atomic coordinates of the crystallized molecule or molecular complex. With the aid of specifically designed computer software, such crystallographic data can be used

- 5 to generate a three dimensional structure of the molecule or molecular complex. Various methods used to generate and refine the three dimensional structure of a crystallized molecule or molecular structure are well known to those skilled in the art, and include, without limitation, multiwavelength anomalous dispersion (MAD), multiple isomorphous replacement, reciprocal space solvent flattening, molecular  
10 replacement, and single isomorphous replacement with anomalous scattering (SIRAS).

The present invention is also directed to an ACP active site of an ACPS-like P-pant transferase, including the active site of ACPS, and comprising the structural coordinates according to Figure 3 of residues ARG14, MET18, ARG21,  
15 GLN22, ARG24, PHE25, ARG28, PHE54, GLU58, ILE68, GLY69, ALA70, SER73 and PHE74 from one monomer of ACPS, and residue ARG45 from a second monomer of ACPS, in each case  $\pm$  a root mean square deviation from the backbone atoms of said amino acids of not more than 1.5 $\text{\AA}$ , or more preferably not more than 1.0 $\text{\AA}$ , or most preferably, not more than 0.5 $\text{\AA}$ . Alternatively, the active site may include, in  
20 addition to the structural coordinates define above, the structural coordinates according to Figure 3 of residues ASP8, ILE9, THR10, GLU11, LEU12, ILE15, ALA16, SER17, ALA19, GLY20, ALA23, ALA26, GLU27, ILE29, ALA51, LYS57, SER61, LYS62, THR66, GLY67, GLN71, LEU72, GLN75, ASP76, ILE77 and LYS93 from the first monomer of ACPS and residues LEU41, SER42, LYS44, GLU48,  
25 GLN83, ASN84, HIS105, THR106 and ALA107 from the second monomer of ACPS, in each case  $\pm$  a root mean square deviation from the backbone atoms of said amino acids of not more than 1.5 $\text{\AA}$ , or more preferably not more than 1.0 $\text{\AA}$ , or most preferably, not more than 0.5 $\text{\AA}$ . Preferably, the ACP active site corresponds

to the configuration of the ACPS molecule in its state of association or inactivation with an agent, and preferably, ACP.

- In addition, the present invention provides the ACPS active site of an ACP that comprises the structural coordinates according to Figure 3 or 5 of residues
- 5 ARG14, LYS29, ASP35, SER36, LEU37, ASP38, VAL40, GLU41, VAL43, MET44, SER47, ASP48, ILE54, SER55, ASP56, GLU57 and GLU60,  $\pm$  a root mean square deviation from the backbone atoms of said amino acids of not more than 1.5 $\text{\AA}$ , or more preferably not more than 1.0 $\text{\AA}$ , or most preferably, not more than 0.5 $\text{\AA}$ .
- Alternatively, the active site further includes, in addition to the coordinates defined
- 10 above, the structural coordinates according to Figure 3 or 5 of residues ASP13, LEU15, PHE28, GLU30, ASP31, LEU32, GLY33, ALA34, VAL39, LEU42, GLU45, LEU46, GLU49, MET52, GLU53, ASP58, ALA59, and LYS61,  $\pm$  a root mean square deviation from the backbone atoms of said amino acids of not more than 1.5 $\text{\AA}$ , or more preferably not more than 1.0 $\text{\AA}$ , or most preferably, not more than 0.5 $\text{\AA}$ .
- 15 Preferably, the ACPS active site corresponds to the configuration of the ACP molecule in its state of association or inactivation with an agent, and preferably, ACPS.

Another aspect of the present invention is directed to a method for identifying an agent that interacts with an active site of an ACPS-ACP complex,

20 comprising the steps of determining an active site of the ACPS-ACP complex from a three dimensional model of the ACPS-ACP complex and performing computer fitting analyses to identify an agent which interacts with said active site. Computer fitting analyses utilize various computer software programs that evaluate the "fit" between the putative active site and the identified agent, by (a) generating a three

25 dimensional model of the putative active site of a molecule or molecular complex using homology modeling or the atomic structural coordinates of the active site, and (b) determining the degree of association between the putative active site and the identified agent. Three dimensional models of the putative active site may be generated using any one of a number of methods known in the art, and include,

but are not limited to, homology modeling as well as computer analysis of raw data generated using crystallographic or spectroscopy data. Computer programs used to generate such three dimensional models and/or perform the necessary fitting analyses include, but are not limited to: GRID (Oxford University, Oxford, UK),

5 MCSS (Molecular Simulations, San Diego, CA), AUTODOCK (Scripps Research Institute, La Jolla, CA), DOCK (University of California, San Francisco, CA), Flo99 (Thistlesoft, Morris Township, NJ), Ludi (Molecular Simulations, San Diego, CA), QUANTA (Molecular Simulations, San Diego, CA), Insight (Molecular Simulations, San Diego, CA), SYBYL (TRIPOS, Inc., St. Louis. MO) and LEAPFROG (TRIPOS,

10 Inc., St. Louis, MO).

The effect of such an agent identified by computer fitting analyses on ACPS-ACP complex activity may be further evaluated by contacting the identified agent with the ACPS-ACP complex and measuring the effect of the agent on ACPS-ACP complex activity. Depending upon the action of the agent on the active site of

15 ACPS-ACP complex, the agent may act either as an inhibitor or activator of ACPS-ACP complex activity. Enzymatic assays may be performed and the results analyzed to determine whether the agent is an inhibitor of ACPS-ACP complex activity (i.e., the agent may reduce or prevent binding affinity between ACPS and ACP, and thereby reduce the level or rate of ACPS-ACP activity compared to

20 baseline), or an activator of ACPS-ACP activity (i.e., the agent may increase binding affinity between ACPS and ACP, and thereby increase the level or rate of ACPS activity compared to baseline). Further tests may be performed to evaluate the effect of the identified agent on bacterial or eukaryotic cell populations, wherein an inhibitor of ACPS-ACP activity inhibits cell viability or reproduction.

25 The present invention is not limited to identifying agents which interact with an active site of the ACPS-ACP complex, but also is directed to a method for identifying an activator or inhibitor of any molecule or molecular complex comprising an ACP binding site or an ACPS binding site. The candidate activator or inhibitor is selected or designed by performing computer fitting

analyses of said candidate agent with the three dimensional model of the molecule or molecular complex comprising the active site. Once the candidate activator or inhibitor is obtained, it may be contacted with the molecule or molecular complex in order to measure the effect the candidate activator or inhibitor has on said

5 molecule or molecular complex.

In this regard, a potential activator or inhibitor of a molecule or molecular complex comprising an ACPS binding site, is obtained by (a) generating a three dimensional model of said molecule or molecular complex comprising an ACPS binding site using the relative structural coordinates according to Figure 3 of residues ARG14, MET18, ARG21, GLN22, ARG24, PHE25, ARG28, PHE54, GLU58, ILE68, GLY69, ALA70, SER73 and PHE74 from a first monomer of ACPS, and residue ARG45 from a second monomer of ACPS, and (b) selecting or designing a candidate activator or inhibitor by performing computer fitting analysis of the candidate activator or inhibitor with the three dimensional model generated in step 10 15 (a). In another embodiment, the relative structural coordinates further include the relative structural coordinates according to Figure 3 of residues ASP8, ILE9, THR10, GLU11, LEU12, ILE15, ALA16, SER17, ALA19, GLY20, ALA23, ALA26, GLU27, ILE29, ALA51, LYS57, SER61, LYS62, THR66, GLY67, GLN71, LEU72, GLN75, ASP76, ILE77 and LYS93 from said first monomer of ACPS and residues 20 25 LEU41, SER42, LYS44, GLU48, GLN83, ASN84, HIS105, THR106 and ALA107 from said second monomer of ACPS. In each case, the  $\pm$  a root mean square deviation from the backbone atoms of the amino acids is not more than 1.5 $\text{\AA}$ , preferably not more than 1.0 $\text{\AA}$ , and most preferably is not more than 0.5 $\text{\AA}$ .

A potential activator or inhibitor of a molecule or molecular complex 25 comprising an ACPS binding site, may be obtained by (a) generating a three dimensional model of said molecule or molecular complex comprising an ACPS binding site using the relative structural coordinates according to Figure 3 or 5 of residues ARG14, LYS29, ASP35, SER36, LEU37, ASP38, VAL40, GLU41, VAL43, MET44, GLU47, ASP48, ILE54, SER55, ASP56, GLU57 and GLU60, and (b)

selecting or designing a candidate activator or inhibitor by performing computer fitting analysis of the candidate activator or inhibitor with the three dimensional model generated in step (a). In another embodiment, the relative structural coordinates further include the relative structural coordinates according to Figure 3

- 5 or 5 of residues ASP13, LEU15, PHE28, GLU30, ASP31, LEU32, GLY33, ALA34, VAL39, LEU42, GLU45, LEU46, GLU49, MET52, GLU53, ASP58, ALA59, and LYS61. In each case, the  $\pm$  a root mean square deviation from the backbone atoms of the amino acids is not more than 1.5 $\text{\AA}$ , preferably not more than 1.0 $\text{\AA}$ , and most preferably is not more than 0.5 $\text{\AA}$ .

10 In addition, the invention provides a solution comprising *B. subtilis* ACP having a three dimensional structure defined by the structural coordinates of Figure 5,  $\pm$  a root mean square deviation from the backbone atoms of said amino acids of not more than 1.5 $\text{\AA}$ , more preferably not more than 1.0 $\text{\AA}$ , and most preferably not more than 0.5 $\text{\AA}$ . Also provided by the invention is any active site of  
15 *B. subtilis* ACP that is defined by the structural coordinates of Figure 5,  $\pm$  a root mean square deviation from the backbone atoms of said amino acids of not more than 1.5 $\text{\AA}$ , more preferably not more than 1.0 $\text{\AA}$ , and most preferably not more than 0.5 $\text{\AA}$ . In addition, the invention provides a method for identifying an agent that interacts with any active site of *B. subtilis* ACP, comprising the steps of  
20 determining a putative active site of ACP from a three dimensional model of the ACP, and performing various computer fitting analyses to identify an agent which interacts with the putative active site. Again, such agents may act as inhibitors or activators of ACP activity, as determined by obtaining the identified agent, contacting the same with ACP, and measuring the agent's effect on ACP activity. In  
25 the preferred embodiment, the three dimensional structure of *B. subtilis* ACP is defined by the relative structural coordinates of Figure 5,  $\pm$  a root mean square deviation from the backbone atoms of said amino acids of not more than 1.5 $\text{\AA}$ , or more preferably not more than 1.0 $\text{\AA}$ , or most preferably, not more than 0.5 $\text{\AA}$ . The use of the NMR solution structure of ACP for the identification of inhibitor binding

sites on ACP, for the determination of the solution structure of ACP-inhibitor complexes, and for inhibitor design, is described further below in Examples 3-5.

Various molecular analysis and rational drug design techniques are further disclosed in U.S. Patent Nos. 5,834,228, 5,939,528 and 5,865,116, as well

- 5 as in PCT Application No. PCT/US98/16879, published WO 99/09148, the contents of which are hereby incorporated by reference.

The present invention is also directed to the agents, activators or inhibitors identified using the foregoing methods. Such agents, activators or inhibitors may be a protein, polypeptide, peptide, nucleic acid, including DNA or

- 10 RNA, molecule, compound, antibiotic or drug.

Finally, the present invention is further directed to a method for determining the three dimensional structure of a molecule or molecular complex whose structure is unknown, comprising the steps of obtaining crystals of the molecule or molecular complex whose structure is unknown and generating X-ray

- 15 diffraction data from the crystallized molecule or molecular complex. The X-ray diffraction data from the molecule or molecular complex is then compared with the known three dimensional structure determined from the ACPS-ACP crystals of the present invention. Then, the known three dimensional structure determined from the crystals of the present invention is "conformed" using molecular replacement  
20 analysis to the X-ray diffraction data from the crystallized molecule or molecular complex. Alternatively, spectroscopic data or homology modeling may be used to generate a putative three dimensional structure for the molecule or molecular complex, and the putative structure is refined by conformation to the known three dimensional structure determined from the ACPS-ACP crystals of the present  
25 invention.

The present invention may be better understood by reference to the following non-limiting Examples. The following Examples are presented in order to more fully illustrate the preferred embodiments of the invention, and should in no way be construed as limiting the scope of the present invention.

Example 1

Crystal Structure of ACPS/ACP Complex

1. Material and Methods

Crystallization of ACPS with ACP. Purified ACP and ACPS were mixed at a 1:1.1

5 molar ratio and the mixture was loaded onto a gel filtration column. The resulting purified complex was dialyzed against a solution containing 50mM Bis-Tris pH 6.4, 100mM NaCl, 10mM MgCl<sub>2</sub>, and 10mM DTT before concentrating the complex to ~10 mg/mL. Crystallization conditions for the ACP/ACPS complex were also determined using the sparse matrix screens available from both Hampton Research 10 and Emerald Biostructures. Screens were set up with 2μL drops at both 18°C and 4°C. Optimization of a crystalline hit (2M Potassium Formate, 20% PEG 3350) gave diffraction quality rod shaped crystals. Crystals could be obtained between 0.15M and 0.3M Potassium Formate and between 15 and 23% PEG 3350. The rate of growth seriously affected the quality of crystals with the optimal crystals being 15 formed between 8 and 12 days after setup. The crystals were grown with a 1:2 drop ratio of protein to well solution at 18°C. These crystals belonged to space group C222<sub>1</sub> with unit cell parameters a=78.46, b=122.03, c=136.77Å and contained three molecules of ACPS and three molecules of ACP in the asymmetric unit.

20 Data Collection. Data from the ACP/ACPS complex crystals were collected using a R-Axis IV mounted on a Rigaku RUH2R rotating anode operating at 5 kW from a single crystal, cooled to -180°C. The data to 2.3Å were collected for the ACP/ACPS complex crystal using one-degree oscillations. The data were processed using DENZO and Scalepack [23] and the statistics from refinement are given in Table 2.

25 Model Building and Refinement. The structure of the ACP/ACPS complex was solved by molecular replacement using the program AMORE[24], with the trimer of ACPS as found in the ACPS/CoA structure as the probe. Prior to refinement,

10% of the data were randomly selected and designated as a  $R_{free}$  test set to monitor the progress of the refinement. The structure of the ACPS trimer was then rebuilt using the X-BUILD feature in Quanta utilizing a series of omit maps. During this rebuilding, extra density was found in each active site that sharpened after 5 each cycle of rebuilding. When the ACPS molecules had been rebuilt, the NMR structure of the *B. Subtilis* ACP was rotated into the density found in the active site. As a result of a large domain shift, a consequence of binding to ACPS, there were enough differences between the NMR structure and the X-Ray data that precluded using the NMR model as the starting point for refinement. Instead, the location of 10 methionine 44 was noted from the NMR structure and the remainder of the ACP molecule was built into density using omit maps from that residue. Reference to the NMR structure as a source of secondary structure information allowed the structure of the three ACP molecules to be built into the electron density rapidly.

When roughly 80% of the ACP had been built into density, that 15 ACP/ACPS model was then used as the initial model for refinement using the program CNS [25]. Following six cycles of refining and rebuilding the refinement converged with a model which contained 3 molecules of ACPS, 3 molecules of ACPS and 117 solvent molecules at an  $R_{cryst}$  of 22.9% and  $R_{free}$  of 28.0%. The refinement statistics are given in Table 3.

20 **2. Results and Discussion**

Needle-like crystals ( $0.1 \times 0.1 \times 0.5\text{mm}$ ) were grown using the hanging drop method from an equal molar solution of ACP and ACPS. These crystals belong to space group C222<sub>1</sub> with unit cell parameters  $a=78.46$ ,  $b=122.03$ ,  $c=136.77\text{\AA}$  and diffract to  $2.3\text{\AA}$  using a R-Axis IV mounted on a Rigaku 25 RUH2R rotating anode operating at 5kW. These cell dimensions correspond to the asymmetric unit containing 3 molecules of ACPS and 3 molecules of ACP. The sequence of the ACP and ACPS used in obtaining these crystals is shown in Figure

1. The phosphopantetheinyl group that is attached to the O<sup>γ</sup> of Ser-36 from ACP is not indicated in this figure.

The contacts between holo-ACP and ACPS are predominately hydrophilic in nature with almost all of the interactions occurring between helix  $\alpha$ 1 of ACPS and helix  $\alpha$ 2 of ACP. There are only two significant hydrophobic contacts and these both involve residues (Leu-37 and Met-44) from ACP protruding into hydrophobic pockets on ACPS. Leu-37 extends into a pocket formed by Met-18, Phe-25, Phe-54 and Ile-15 on ACPS while Met-44 binds in a pocket formed by Phe-25 and the aliphatic portion of the side chains from Arg-28 and Gln-22. Table 1 details the hydrophilic interactions.

Examination of this structure suggests that a key residue in the binding of ACP to ACPS is Arg-14 from ACPS. Arg-14 forms a salt bridge with the residue just before the reactive serine (Asp-35) of ACP and is involved in hydrogen bonding with Asp-38, two residues after the reactive serine. These interactions serve to position the ACP molecule so that one end of helix  $\alpha$ 2 from ACP is placed at the bottom of the active site and correctly orients Ser-36. As shown in Figure 2, Arg-14 is conserved in all ACPS proteins except that from Mycobacterium in which it is an aspartic acid. Another arginine, Arg-21, of ACPS forms a salt bridge with Glu-41 from ACP. The other end of helix  $\alpha$ 2 is positioned by the interactions of Arg-24 and Gln-22 from ACPS with Asp-48 of ACP. These interactions, along with the two hydrophobic "keys" described above, lock the ACP into place.

When the structure of ACPS/CoA and ACPS/ACP are superimposed (not shown), a loop consisting of residues 64 to 78 enlarges the active site by shifting 2 Å to accommodate helix  $\alpha$ 3 from ACP. Additionally, the dipole of the  $\alpha$ 2 helix of ACP is directed at the phosphate of the CoA that is to be transferred to ACP.

Since there is a significant rearrangement of ACP upon binding to ACPS and there are only limited interactions between the ACP and ACPS, it is not surprising that the B-values indicate the ACP molecules are very mobile. The

average B of the main chain atoms of the three ACPS molecules is  $40.1\text{\AA}^3$  while that of the three ACP molecules is  $72.3\text{\AA}^3$ .

**Table 1.** Hydrophilic Interactions between ACP and ACPS

	ACP Residue	ACPS Residue	Distance (Å)
	Hydrophilic		
5	9 LYS NZ	308 GLU OE1	3.15*
	35 ASP OD1	214 ARG NH2	2.81
	35 ASP OD2	214 ARG NH1	2.50
	35 ASP OD2	214 ARG NH2	3.05
	38 ASP OD1	214 ARG NH2	3.05
	38 ASP OD2	214 ARG NH2	3.20
10	41 GLU OE1	221 ARG NH2	2.66
	41 GLU OE2	221 ARG NE	2.91
	48 ASP OD1	224 ARG NH1	2.95
	54 ILE O	228 ARG NH2	2.60
	56 ASP OD2	273 SER OG	2.50
	56 ASP OD2	274 PHE N	2.85
15	60 GLU OE2	270 ALA N	2.97

\* denotes a symmetry related molecule

**Table 2.** Residues of ACPS from Figure 1 that were modeled as alanine due to poor electron density beyond Cβ for ACPS long chain residue

	<u>Amino Acid</u>	<u>Chain A</u>	<u>Chain B</u>	<u>Chain C</u>
20	Lys13	Ala	Ala	Lys
	Arg21	Ala	Arg	Ala
	Arg32	Ala	Arg	Ala
	Glu40	Ala	Ala	Glu
	Glu43	Glu	Ala	Ala
	Arg45	Arg	Ala	Arg
	Arg70	Arg	Ala	Ala
	Lys81	Lys	Ala	Lys
	Gln83	Ala	Gln	Gln
	Lys86	Lys	Ala	Lys
30	Gln96	Gln	Gln	Ala
	Lys107	Lys	Ala	Ala

**Table 3.** Statistics for Data Collection, Phase Determination, and Refinement

	<u>Data Collection</u>	<u>ACP/ACPS</u>
5	Wavelength (Å)	$\lambda = 1.54$
	resolution range(Å)	15-2.3
	$R_{\text{merge}}^{\text{a}}$	5.7%(56.0)
	% complete	97.7(94.5)
	total reflections	270151
10	unique reflections	29694
	$I/\sigma(I)$	26.6(3.5)
	<u>Model Refinement</u>	<u>ACP/ACPS</u>
	Maximum Resolution(Å)	2.3
15	$R_{\text{work}}^{\text{b}} (%)$	22.9
	$R_{\text{free}} (%)$	28.0
	$\langle B \text{ value} \rangle (\text{\AA}^3)$	52.3
	R.m.s. Deviations from ideal geometry for	
	Bonds(Å)	0.0156
20	Angles(°)	1.80
	$B$ values ( $\text{\AA}^2$ )	2.054
	Non-hydrogen Protein Atoms	6972
	Water Molecules	117
	Ions	none
25	Other Molecules	none

---

<sup>a</sup>  $R_{\text{merge}} = \frac{1}{2}\bar{I}_h - \langle I_h \rangle^{1/2} / \bar{I}_h$ , where  $\langle I_h \rangle$  is the average intensity over symmetry equivalents. Number in parentheses reflect statistics for the last shell

<sup>b</sup>  $R_{\text{work}} = \frac{1}{2}\sqrt{\frac{1}{2}\mathbf{F}_{\text{obs}}^{1/2} - \frac{1}{2}\mathbf{F}_{\text{calc}}^{1/2}} / \sqrt{\frac{1}{2}\mathbf{F}_{\text{obs}}^{1/2}}$ ,  $R_{\text{free}}$  is equivalent to  $R_{\text{work}}$ , but calculated for a randomly chosen 5% (or 10%) of reflections omitted from the refinement process.

Table 4.

Residues from ACPS which are within 4Å of ACP.

From one molecule of ACPS:

- Arg-14, Met-18, Arg-21, Gln-22, Arg-24, Phe-25, Arg-28, Phe-54, Glu-58, Ile-68,  
5 Gly-69, Ala-70, Ser-73, Phe-74

From a second molecule of ACPS:

Arg-45

Residues from ACP which are within 4Å of the ACPS dimer.

- Arg-14, Lys-29, Asp-35, Ser-36, Leu-37, Asp-38, Val-40, Glu-41, Val-43, Met-44,  
10 Glu-47, Asp-48, Ile-54, Ser-55, Asp-56, Glu-57, Glu-60

Table 5.

Residues from ACPS which are within 8Å of ACP.

From one molecule of ACPS:

- Asp-8, Ile-9, Thr-10, Glu-11, Leu-12, Arg-14, Ile-15, Ala-16, Ser-17, Met-18 Ala-19,  
15 Gly-20, Arg-21, Gln-22, Ala-23, Arg-24, Phe-25, Ala-26, Glu-27, Arg-28, Ile-29, Ala-  
51, Phe-54, Lys-57, Glu-58, Ser-61, Lys-62, Thr-66, Gly-67, Ile-68, Gly-69, Ala-70,  
Gln-71, Leu-72, Ser-73, Phe-74, Gln-75, Asp-76, Ile-77, Lys-93

From a second molecule of ACPS:

Leu-41, Ser-42, Lys-44, Arg-45, Glu-48, Gln-83, Asn-84, His-105, Thr-106, Ala-107

- 20 Residues from ACP which are within 8Å of the ACPS dimer.

Asp-13, Arg-14, Leu-15, Phe-28, Lys-29, Glu-30, Asp-31, Leu-32, Gly-33, Ala-34,  
Asp-35, Ser-36, Leu-37, Asp-38, Val-39, Val-40, Glu-41, Leu-42, Val-43, Met-44,  
Glu-45, Leu-46, Glu-47, Asp-48, Glu-49, Met-52, Glu-53, Ile-54, Ser-55, Asp-56,  
Glu-57, Asp-58, Ala-59, Glu-60, Lys-61

Example 2

Determination of NMR Solution Structure of ACP

1. Material and Methods

*B. subtilis* ACP Sample Preparation. The uniform <sup>15</sup>N and <sup>13</sup>C-labeled *B. subtilis*

- 5 ACP was cloned into pGEX-6P-1 vector and expressed in *E. coli* strain BL21DE3 (pLysS) similar to the conditions previously reported for expression of ACPS [26], except that 0.5 mM IPTG was used for induction. Purification was done using the following procedure. Typically, 20 grams of cell pellet expressing GST-ACP fusion protein was resuspended in 300 ml breaking buffer consisting of 50 mM Tris·Cl (pH 10 8.0), 300 mM NaCl, 10 mM MgCl<sub>2</sub> and 2 mM of freshly prepared MnCl<sub>2</sub>. Protease inhibitor tablets (Boehringer Mannheim GmbH, Mannheim, Germany), RNase H and DNase I (Sigma Chemical Co., St. Louis, MO) were added to the solution to prevent protease activity and to decrease viscosity of the solution. The cells were lysed by three passages through a Microfluidizer and the whole lysate was rocked 15 at room temperature for one hour to enable the conversion of holo-ACP to apo-ACP by an endogenous ACP hydrolase from *E. coli* [27]. Once the incubation was finished, the lysate was centrifuged at 15,000 g for 20 minutes at 4°C to remove the cell debris. Glutathione sepharose 4B resin (Amersham Pharmacia Biotech, Piscataway, NJ) equilibrated with the same breaking buffer was added to the clear 20 supernatent to a rough ratio of 1 ml resin slurry per 8 mg of GST fusion protein. The mixture was incubated at 4°C for one hour by gentle rocking and centrifuged at 3,000 g for 10 minutes to remove excess supernatent prior to packing the resin into a suitable column. The column was then washed with 5 column volume of washing buffer containing 50mM Tris·Cl (pH 8.0), 10 mM MgCl<sub>2</sub>, 5 mM DTT. The GST-ACP 25 was eluted with wash buffer plus 60 mM freshly prepared reduced glutathione. The resulting GST-ACP solution was dialyzed overnight with Prescission Protease Cleavage buffer consisting of 50 mM Tris·Cl (pH 8.0), 150 mM NaCl, 1 mM EDTA and 1 mM DTT. The fusion protein was cleaved with Prescission Protease (Amersham Pharmacia Biotech, Piscataway, NJ ) at room temperature for three

hours at a ratio of 1U enzyme per 500 µg protein. The resulting protein mixture was loaded onto a MonoQ HR16/10 column (Amersham Pharmacia Biotech) equilibrated with 50 mM Tris·Cl; pH 8.0, 150 mM NaCl and 10 mM MgCl<sub>2</sub>.

NMR Data Collection. The NMR sample is a mixture of <sup>15</sup>N-, <sup>13</sup>C-double labeled

- 5 Apo- and Holo-ACP in 50 mM Bis-Tris ( pH 6.4), 100 mM NaCl, 10 mM MgCl<sub>2</sub> and 10 mM DTT with 0.02% NaN<sub>3</sub> in 5% D<sub>2</sub>O/95% H<sub>2</sub>O solution. The protein concentration was < 1mM.

All spectra were recorded at 25° C on Varian Unity<sup>+</sup> 600 spectrometer equipped with triple-resonance <sup>1</sup>H/<sup>13</sup>C/<sup>15</sup>N probe and an actively shielded z-

- 10 gradient pulsed field accessories. 2D-<sup>1</sup>H-<sup>15</sup>N HSQC and all triple-resonance 3D experiments were recorded with the enhanced-sensitivity pulsed field gradient approach [28]. This approach provides coherence transfer selection both to improve sensitivity and eliminate artifacts as well as for solvent suppression.

Data sets were typically processed and displayed on SGI workstation  
15 using the program packages NMRDraw and NMRPipe [29]. A skewed 60° phase-shifted sine-bell function and a single zero-filling was used in each of the all three dimensions prior to Fourier transformation. For triple-resonance 3D experiments, the time domain was extended by a factor of two using forward-backward linear prediction in the <sup>15</sup>N (t2) dimension and for constant-time <sup>1</sup>H-<sup>13</sup>C correlation  
20 experiments, mirror image linear prediction was used prior to zero-filling to the double time-domain data points [30]. The programs PIPP and STAPP [31] were used for data analysis and semi-automatic assignments [30].

The complete assignments (>95% ) of the <sup>1</sup>H, <sup>15</sup>N and <sup>13</sup>C resonances were based on the following experiments: CBCA(CO)NNH, HNCACB,

- 25 C(CC)TOCSY\_NNH, H(CC)TOCSY\_NNH, HAHB(CBCACO)NNH [28,32]. 2D <sup>13</sup>C (methyl)-<sup>1</sup>H HSQC and methyl relay experiments used for auxiliary methyl assignments of Ile, Val and Leu residues [33-35]. Some ambiguous resonances were further confirmed by simultaneous <sup>15</sup>N/<sup>13</sup>C-edited NOESY [36].

*B. subtilis* ACP Structure Calculation. The NMR solution structure is based on interproton distance constraints converted from observed NOEs in both the <sup>15</sup>N-edited NOESY [37,38] and simultaneous <sup>15</sup>N/<sup>13</sup>C-edited NOESY experiments [36]. The NOEs were classified as either strong (1.8-2.7 Å), medium (1.8-3.3 Å) or weak 5 (1.8-5.5 Å) constraints.  $\phi$  and  $\psi$  torsion angle constraints were obtained from <sup>15</sup>N, H $\alpha$ , C $\alpha$  and C $\beta$  chemical shifts using the TALOS program [39]. Upper distance limits for distances involving methyl protons and non-stereospecifically assigned methylene protons were corrected appropriately for center averaging [40], and an additional 0.5 Å was added to upper distance limits for NOEs involving methyl 10 protons [41,42].

The structures were calculated using the hybrid distance geometry-dynamical simulated annealing method of Nilges et al. (1988) [43] with minor modifications [44] using the program XPLOR [45], adapted to incorporate pseudopotential secondary <sup>13</sup>C $\alpha$ /<sup>13</sup>C $\beta$  chemical shift restraints [46] and a 15 conformational database potential [47,48]. The target function that is minimized during restrained minimization and simulated annealing comprises only quadratic harmonic terms for covalent geometry and secondary <sup>13</sup>C $\alpha$ /<sup>13</sup>C $\beta$  chemical shift restraints, square-well quadratic potentials for the experimental distance and torsion angle restraints, and a quartic van der Waals term for non-bonded contacts. 20 All peptide bonds were constrained to be planar and trans. There were no hydrogen-bonding, electrostatic or 6-12 Lennard-Jones empirical potential energy terms in the target function.

The structure of *B. subtilis* ACP was determined from a total of 1050 distance constraints comprising 337 intra-residue, 231 sequential, 188 medium, 25 and 240 long range distance constraints, 54 hydrogen bond constraints and 92 torsion angles constraints comprised of 46  $\phi$  and 46  $\psi$  dihedral constraints. The hydrogen bond constraints were based on the observation of slow exchanging NH protons in a D<sub>2</sub>O solution monitored by an <sup>1</sup>H-<sup>15</sup>N HSQC spectrum.

The final ensemble of 22 structures contained no distance constraint violations greater than 0.2 Å and no torsion angle constraint violations greater than 2°. The NMR structures are well defined. This is evident by the atomic rms distribution of the 22 simulated annealing structures about the mean coordinate

5 positions where the backbone and all atom rms is 0.45 Å and 0.93 Å, respectively. For residues only in secondary structure regions, the backbone and all atom rms is 0.35 Å and 0.84 Å, respectively. The *B. subtilis* ACP NMR structure is consistent with a good quality structure based on PROCHECK and Ramachandran analysis [49,50]. A Ramachandran plot of the minimized average structure shows a total of

10 83.1% of the residues are in the most favored region, 12.7% in the additional allowed, and 2.8% in the generously allowed regions with only one residue (Val17) in a disallowed region (based on residues 6-81 of ACP). Val17 is located in a long loop between helices 1 and 2 that corresponds to a very flexible region of the protein. PROCHECK analysis indicates an overall G-factor of -0.23, a hydrogen

15 bond energy of 0.9 and only 2 bad contacts.

## 2. Results and Discussion

Introduction. The biosynthesis of fatty acids consists of a series of reactions catalyzed by specific enzymatic activities [51]. The organization of the enzymatic activity is significantly different between eukaryotic cells and prokaryotic and plants cells. In eukaryotic cells large multifunctional enzymes exist with distinct domains associated with a particular function. Conversely, in prokaryotic and plant cells, the various enzymatic activities is associated with individual proteins that are loosely associated with each other. Acyl carrier protein (ACP) is a discrete small acid protein (9 KDa) in prokaryotic and plant cells that plays an essential role in fatty acid biosynthesis; whereas, ACP is a subunit of fatty acid synthetase (FAS) in animal tissue. ACP is the carrier of fatty acids during fatty acid biosynthesis in prokaryotic and plant cells and is responsible for acyl group activation [51-53].

A unique feature of ACP is the presence of the 4'-phosphopantetheine (P-pant) prosthetic group. The P-pant moiety is attached through a phosphodiester linkage to a specific conserved serine residue found in all ACPs. ACP exists in both an active (holo) and inactive (apo) form where activation of ACP is mediated by

- 5 Holo-acyl carrier protein synthase (ACPS). ACPS transfers the P-pant moiety from CoA to Ser-36 of Apo-ACP to produce holo-ACP and 3',5'-ADP in a Mg<sup>+2</sup> -dependent reaction. During biosynthesis of a long-chain fatty acid, the fatty acid chain is attached to ACP via a thioester linkage to the terminal cysteamine thiol of the P-pant prosthetic group where the fatty acid chain is then elongated by the fatty acid  
10 synthetase system. A potential function of the P-pant prosthetic group is to act as a tether to transfer the growing fatty acid chains between the various enzymes or active sites in the FAS system.

ACP is a central component and plays a fundamental role in fatty acid and other biosynthetic pathways that require acyl transfer steps [54, 55-58]. The

- 15 activation of ACP by ACPS is critical to this function where ACPS was identified as critical for the viability of *E. coli* [59,60]. Furthermore both ACP and ACPS are viable targets for a drug discovery program since the enzymes are essentially unique to prokaryotic cells. Since the activation of ACP is mediated by its interaction with ACPS, interfering with either the activity of ACPS or the binding  
20 interaction of ACPS with ACP may prove to be a valuable approach for developing novel antibiotics.

NMR Data. NMR data was collected on both the apo- and holo- forms of ACP.

While the NMR spectra indicate distinct chemical shifts for the NH proton and amide-<sup>15</sup>N resonances for residues in the vicinity of the 4'-PP prosthetic group, the

- 25 NMR data indicate that the structures for apo-ACP and holo-ACP are effectively identical.

Uniqueness of the *B. subtilis* ACP NMR Structure. Structures for *E. coli* and *Streptomyces coelicolor* A3(2) ACP were reported in the literature prior to initiation of our efforts on the structure determination of *B. subtilis* ACP [61-63]. Amino acid sequence alignments indicate that *E. coli* ACP is highly homologous to *B. subtilis*

- 5 ACP where 53 of 76 residues are identical residue types (46) and identical residue classes (7). Comparison of *Streptomyces coelicolor* A3(2) ACP with *B. subtilis* ACP indicate 38 of 76 residues are identical residue types (17) and identical residue classes (21). The overall sequence homology suggests that the three proteins should have a similar global fold (Figure 4).

10 Comparison of the published structures for *E. coli* and *Streptomyces coelicolor* A3(2) ACP with *B. subtilis* ACP indicate similar secondary structure elements for the three proteins. The overall ACP structure consists of a four  $\alpha$ -helical bundle where three  $\alpha$ -helices are relatively long (6-15 residues) and one helix is short (0-6 residues). Despite the similarity in the secondary structure

- 15 features the global fold for the three ACP structures is distinct. This is readily apparent by the superposition of the average-minimized three-dimensional structures for the three proteins (not shown). The atomic rms deviation of the C $\alpha$  trace between *E. coli* and *B. subtilis* ACP is 2.32 Å. Similarly, the deviation of the C $\alpha$  trace between *Streptomyces coelicolor* A3(2) and *B. subtilis* ACP is 2.31 Å.

20 Although the previous structures of *E. coli* ACP and *Streptomyces coelicolor* A3(2) are of poor quality, the extremely large rms differences between *E. coli* ACP, *Streptomyces coelicolor* A3(2) and *B. subtilis* ACP indicate that each structure is relatively unique and that it would not be possible to predict the structure of *B. subtilis* ACP from the structures of *E. coli* ACP and *Streptomyces coelicolor* A3(2).

25 The observed large rms deviations between the three ACPS structures are located mainly in the short  $\alpha$ -helix 3 and the long loop region between  $\alpha$ -helix 1 and 2. The short  $\alpha$ -helix 3 is not present in some models of both *E. coli* and *Streptomyces coelicolor* A3(2) ACP and is not present in the average minimized *Streptomyces coelicolor* A3(2) ACP structure. Some of the observed differences

between the *B. subtilis* ACP structure and both the *E. coli* and *Streptomyces coelicolor* A3(2) ACP structures result from unusual features of the *E. coli* and *Streptomyces coelicolor* A3(2) ACP structures. An example of an unusual feature is the presence of a large kink in  $\alpha$ -helix 1 for *E. coli* ACP that results in this helix being extremely distorted. The observation of distinct structures for the three ACP proteins is unexpected given the reasonable sequence homology and the obvious fact that the proteins are functionally identical. A potential cause for the structural difference may be a function of the structure determination process instead of a difference that may be attributed to the origin of the proteins.

- 10           The available structural information for ACP has been obtained by NMR methodologies over a span of ~12 years. During this time-period NMR technology has been vastly improved resulting in the ability to obtain high-resolution structures of increasingly larger proteins [64-66]. As a result, the methodology applied to determining the *B. subtilis* ACP structure is inherently superior to the techniques used for the *E. coli* and *Streptomyces coelicolor* A3(2) ACP structures. Invariably, the precision and accuracy of a protein structure determined by NMR is dependent on the number and reliability of the structural constraints interpreted from the NMR data [64,67]. The inherent reliability of the interpretation of the structural constraints is dependent on the number of available constraints. This relationship exists since a given structure has to be consistent with all the available constraints. So, the more constraints that are available for determining a structure the higher the likelihood that erroneous data will be identified by being inconsistent with the abundance of correct data. Additionally, the nature of the structural constraint is critical in relationship to the accuracy of the overall structure. Intra-residue constraints convey a localized structural effect usually contributing to the residues torsion angles whereas long-range inter-residue constraints will determine the overall fold of the protein. Therefore, a protein structure with an abundance of intra-residue constraints and a minimal number of long-range constraints will result in a relatively low-resolution structure.

The structures for *E. coli* and *Streptomyces coelicolor* A3(2) ACP were based on a minimal number of distance constraints, especially long-range distance constraints, relative to the *B. subtilis* ACP structure. *E. coli* ACP (77 residues) structure was based on a total of 478 distance constraints comprising 30 H-bond distance constraints, 101 intra-residue distance constraints and 205 sequential, 87 short-range and 55 long-range inter-residue constraints. The average number of distance constraints was only 6.2 constraints per residue. Similarly, the 5 *Streptomyces coelicolor* A3(2) ACP (86 residues) structure was based on a total of 747 distance constraints comprising 48 H-bond distance constraints, 240 intra-residue constraints, 235 sequential, 131 short-range and 93 long-range distance 10 constraints. The average number of distance constraints for *Streptomyces coelicolor* A3(2) ACP was only 8.7 constraints per residues. Conversely, our *B. subtilis* ACP (76 residues) structure is based on a total of 1050 distance constraints with an average of 13.8 constraints per residue. Similarly, the *B. subtilis* ACP structure is 15 based on more  $\phi$ ,  $\psi$  dihedral angle constraints relative to both *E. coli* and *Streptomyces coelicolor* A3(2) ACP. A total of 92  $\phi$  and  $\psi$  dihedral angle constraints were used for the *B. subtilis* ACP structure compared to 54 and 63 for the *E. coli* and *Streptomyces coelicolor* A3(2) ACP structures, respectively. In addition, the *B. subtilis* ACP structure was refined using both C $\alpha$ /C $\beta$  chemical shifts 20 constraints and a conformational database potential which were not used for determining the *E. coli* and *Streptomyces coelicolor* A3(2) ACP structures. In addition to the number of constraints, the quality of the ACP structures is also reflected by the rms difference between each structure in the ensemble relative to the average structure. Typically, a high resolution NMR structure exhibits a 25 backbone rms of < 0.5 Å [64]. As apparent in Table 5, the structures for *E. coli* and *Streptomyces coelicolor* A3(2) ACP have extremely high rms values suggestive of a low to poor quality structure, whereas, *B. subtilis* ACP conforms to a rms value consistent with a high quality structure.

**Table 5:** Atomic rms Differences (Å) <sup>a</sup>

		<i>E. coli</i> ACP	<i>Streptomyces coelicolor</i> A3(2) ACP <sup>b</sup>	<i>B. subtilis</i> ACP
All Residues				
	Backbone	2.3	1.47	0.45
5	All atoms	3.3	1.84	0.93
Secondary Structure				
	Backbone	N.D.	1.01	0.35
	All atoms	N.D.	1.45	0.84

<sup>a</sup>The NMR ensemble for the *E. coli*, *Streptomyces coelicolor* A3(2) and *B. subtilis* ACP structures consist of 7, 24 and 22; respectively. <sup>b</sup>Only residues 5-86 were used for the rms.

There is additional evidence that indicates that the previous structural efforts related to ACP were problematic which may imply that the previous ACP structures may be inaccurate relative to the structure of *B. subtilis* ACP. The NMR structure for *E. coli* ACP was published in 1988, further modified in 1990 and finally released by the PDB in 1993 (PDB:1ACP). In fact, two separate models for *E. coli* ACP were deposited in the PDB, where one model is described as "Not Energetically Ideal" and the authors suggest multiple conformers. Structural information for Spinach ACP and the nodulation protein NodF from *Rhizobium leguminosarum*, which shares homology with ACP were also published, but the NMR data was of too low a quality to determine and release a three dimensional structure [68,69]. These results clearly suggest an inherent technical difficulty that was encountered with the previous ACPs structures that was not a factor in the *B. subtilis* ACP structure.

- The uniqueness of the three structures and more critically the inherent value and accuracy of the *B. subtilis* ACP was also apparent from the molecular replacement efforts for solving the X-ray structure of the *B. subtilis* ACP-ACPS complex. It was *not* possible to solve the X-ray structure of ACP in the *B.*
- 5     *subtilis* ACP-ACPS complex using the *E. coli* ACP structure. A solution to the X-ray structure of ACP in the *B. subtilis* ACP-ACPS complex was only obtained when the NMR *B. subtilis* ACP structure was used as part of a molecular replacement approach.

### Example 3

10     Identification of Inhibitor Binding Sites on ACP

Inhibitors of the ACPS conversion of apo-ACP to holo-ACP were analyzed for direct binding to either ACP or ACPS by NMR. Inhibitor binding to ACP was monitored by chemical shift perturbations in a 2D  $^1\text{H}$ - $^{15}\text{N}$  HSQC spectra. The observation of chemical shift perturbations in a 2D  $^1\text{H}$ - $^{15}\text{N}$  HSQC spectra indicate both an interaction between ACP and the inhibitor and the location of the inhibitor binding site. The NMR assignments for free ACP was utilized to identify which residues have changed in the ACP-inhibitor complex. Further identification of the binding site was obtained by superimposing the perturbed residues onto the NMR structure of ACP. All of the residues that experience chemical shift changes in the presence of the inhibitor occur on a loop region corresponding to residues 53-56. This loop is spatially proximal to the conserved serine (S36) that is attached through a phosphodiester linkage to the 4'phosphopantetheine (P-pant) prosthetic group. The identification of the location of the P-pant prosthetic group was determined by chemical shift differences between the apo- and holo- forms of ACP.

15     The proximal location of the potential inhibitor-binding site with the P-pant binding site suggests two possible mechanisms for inhibition of the ACP-ACPS activity. The activity of the inhibitor could be attributed to disruption of the binding of ACP with

ACPS or it may sterically prevent the addition of the P-pant prosthetic group to ACP from CoA.

Specificity for the inhibitor to ACP is also monitored by its ability to bind ACPS. Inhibitor binding to ACPS was monitored by line-width changes in one-dimensional  $^1\text{H}$  titration studies. An effect of the large molecular-weight difference between ACPS and a small molecular inhibitor is the corresponding difference in the observable NMR line-widths. If the small molecule binds ACPS, it will demonstrate an apparent molecular weight similar to ACPS resulting in a dramatic increase in the NMR line-widths for the small molecule. Inhibitors identified to affect the ACP-ACPS activity have been shown to bind either ACP or ACPS.

#### Example 4

##### Use of the ACP NMR Structure to Determine the Solution Structure of ACP-Inhibitor Complexes

When an appropriate ACP inhibitor has been identified, a structure for the ACP complexed to the inhibitor may be determined from the following procedure.

NMR Data Collection. NMR sample preparation and data collection and processing were as described in Example 2, with the addition of the inhibitor in either a molar excess or a 1:1 molar ratio with ACP.

NMR Assignments. The assignments of the  $^1\text{H}$ ,  $^{15}\text{N}$ , and  $^{13}\text{C}$  resonances of ACP in the ACP-inhibitor complex are based on a minimal set of experiments: 2D  $^1\text{H}$ - $^{15}\text{N}$  HSQC, 3D  $^{15}\text{N}$ - edited NOESY [37,38], CBCA(CO)NH [30], C(CO)NH [71], HC(CO)NH, [71], HNHA [72] and HNCA [73].

The nearly complete resonance assignments for ACP provided the starting point for the assignments of ACP in the new inhibitor complex. Three important observations facilitated these assignments and provided a simple “boot-

strap" approach using a minimal set of NMR experiments. First, as apparent by the chemical shift perturbations in a 2D  $^1\text{H}$ - $^{15}\text{N}$  HSQC spectra, >90% of the ACP residues are unperturbed by the presence of the new inhibitor. In fact, for

5 inhibitors that bind ACP in a similar manner the resonance assignments for ACP in the complex will be very comparable and greatly facilitate the assignment process.

This indicates that the majority of the ACP structure is unaffected and that only residues in close proximity to the new inhibitor may incur a significant chemical shift change. Therefore, the backbone assignments of residues in the vicinity of the inhibitor may be obtained by following sequential NOE connectivities in the 3D  $^{15}\text{N}$ -

10 edited NOESY spectra by starting with unaffected residues sequential to perturbed residues.

Second, while significant  $^1\text{H}$  and  $^{15}\text{N}$  chemical shift perturbations occur for residues in the vicinity of the inhibitor, the general NOE pattern may be intact. Simple comparison of the 3D  $^{15}\text{N}$ -edited NOESY spectra of ACP and the new

15 complex may readily identify the sequential and intra-residue NOEs in the ACP:Inhibitor spectra. This provides a straight-forward approach to side-chain  $^1\text{H}$  assignments. Third,  $^{13}\text{C}$  chemical shifts generally do not incur any significant chemical shift perturbations even for residues in close proximity to the new inhibitor.

20 The resonance assignments and bound conformation of the inhibitor in ACP-inhibitor complex are based on the 2D  $^{12}\text{C}$ / $^{12}\text{C}$ -filtered NOESY [74,75], 2D  $^{12}\text{C}$ / $^{12}\text{C}$ -filtered TOCSY [74,75] and  $^{12}\text{C}$ / $^{12}\text{C}$ -filtered COSY experiments [76]. The ACP-inhibitor NMR sample is composed of  $^{13}\text{C}$ / $^{15}\text{N}$  labeled ACP and unlabeled inhibitor. Thus, traditional 2D-NOESY, COSY and TOCSY spectra of the inhibitor in  
25 the presence of ACP were determined from 2D  $^{12}\text{C}$ -filtering experiments [74-76] where only crosspeaks between protons attached to  $^{12}\text{C}$  carbons are observed. This efficiently filters all protein resonances and allows for the straight-forward analysis of the inhibitor spectrum.

The ACP-inhibitor structure is based on the following series of spectra: HNHA [72], HNHB [77], 3D long-range  $^{13}\text{C}$ - $^{13}\text{C}$  correlation [78], coupled CT-HCACO [79,80], HACAHB-COSY [81], 3D  $^{15}\text{N}$ - [37,38] and  $^{13}\text{C}$ -edited NOESY [82,83], 3D  $^{13}\text{C}$ -edited/ $^{12}\text{C}$ -filtered NOESY [84], 2D  $^{12}\text{C}$ / $^{12}\text{C}$ -filtered NOESY [74,75] and  $^{15}\text{N}$ -edited ROESY [85]. The  $^{15}\text{N}$ -edited NOESY,  $^{13}\text{C}$ -edited NOESY, 2D  $^{12}\text{C}$ / $^{12}\text{C}$ -filtered NOESY, 3D  $^{13}\text{C}$ -edited/ $^{12}\text{C}$ -filtered NOESY and  $^{15}\text{N}$ -edited ROESY experiments were collected with 100 msec, 120 msec, 100 msec, 110 msec and 40 msec mixing times, respectively.

The ACP-inhibitor structure is based on the observed intermolecular and intramolecular NOEs from the inhibitor observed in the 3D  $^{15}\text{N}$ -edited NOESY [37,38], 2D  $^{12}\text{C}$ / $^{12}\text{C}$ -filtered NOESY [74,75], 3D  $^{13}\text{C}$ -edited/ $^{12}\text{C}$ -filtered NOESY [84].

Structure Calculations. The structure calculations and distance restraints are used as described in Example 2 with the following modifications. The restraints used for the refinement of the ACP-inhibitor NMR structure are amended with the distance restraints observed between ACP and the inhibitor from the 3D  $^{13}\text{C}$ -edited/ $^{12}\text{C}$ -filtered NOESY and 3D  $^{15}\text{N}$ -edited NOESY experiments and the intra-molecular restraints observed for the inhibitor from the 2D  $^{12}\text{C}$ -filtered NOESY experiment. Additionally, the ACP NMR restraints are modified as appropriate for residues in the vicinity of the active site. This permits the structure of the ACP active site to be determined primarily by the observed inter-molecular NOEs between ACP and the inhibitor. Also, the ACP-inhibitor complex may be refined using the  $^3J_{\text{NH}_\alpha}$  coupling constants determined from the HNHA [72] experiment and secondary  $^{13}\text{C}\alpha$ / $^{13}\text{C}\beta$  chemical shift restraints from the assignments for the complex.

Generation of the bound conformation of the inhibitor followed the general procedure described for ACP in Example 2 with the following modifications. The bound conformation for the inhibitor is generated using QUANTA97 and CHARMM (Molecular Simulations Inc., San Diego) and the XPLOR

topology and parameter files is generated using XPLOR2D [86]. Generation of the bound conformation of the inhibitor follows the following general procedure. The initial inhibitor structure is created using the QUANTA97 2D-sketcher application and is subjected to 500 steps of CHARMM minimization. NOE restraints were

- 5 created using the CHARMM distance/dihedral constraint option. The NOE scaling constant is set to 500 and the structure is subject to an additional 500 steps of CHARMM minimization.

The starting ACP-inhibitor complex structure for the simulated-annealing protocol is then obtained by manually docking the bound conformation  
10 of the inhibitor into the NMR structure determined for ACP using QUANTA97. The inhibitor was then subjected to a 1000 steps of restrained CHARMM minimization using the inhibitor intramolecular and intermolecular NOE restraints while keeping coordinates for ACP fixed. This approach approximates the positioning of the inhibitor in the active site of ACP without distorting the ACP structure. The final  
15 structure is exported as a PDB file and used as the starting point for the standard XPLOR simulated annealing protocol where all residues in the structure are free to move.

#### Example 5

##### Inhibitor Design

- 20 General. There are a number of computational software packages that may be used for the analysis of protein NMR structures. In this case, the software packages Sybyl v.6.4+ to v.6.5+ from Tripos Associates and QUANTA97 (Version 97.1003) and XPLOR (Version 3.840) from MSI were the packages used. Once the coordinates have been determined by NMR a number of steps may be taken as listed below:

- 25 1. The original coordinates are read into the software package and the three-dimensional structure is analyzed graphically. In addition, programs within QUANTA check for the correctness of the NMR coordinates with regard to features such as bond and atom types.

2. The modified (if necessary) structure is energy minimized using the QUANTA/CHARM until all the structural parameters are at their equilibrium/optimal values.

3. The energy minimized structure is superimposed against the 5 original NMR structure to ensure there are no significant deviations between the original and minimized coordinates.

4. The protein-native ligand complex is analyzed, the interactions between the native ligand and the protein are identified. The uncomplexed structure binding site is compared to the complexed structure's binding site for 10 areas which may be exploited by a potential inhibitor.

5. The final protein structure bound to the inhibitor is modified by removing the inhibitor so only the protein and a few residues of the natural ligand are left for analysis of the binding site cavity. The natural ligand residues are docked into the uncomplexed structure's binding site to be used as templates for 15 SYBYL/UNITY database searching.

6. SYBYL/UNITY is used to create excluded volume and distance constrained queries for searching structural databases. Structures qualifying as 'hits' are screened for activity.

7. Once specific inhibitor-protein interactions are determined 20 between new inhibitors and the protein structure, docking studies may be carried out between the different series of in-house inhibitors and ACP. This part gives the initial modeled complexes of new inhibitors with ACP.

To check for the integrity of the modeled new ACP-inhibitor complexes, different procedures may be used. In this case, constrained 25 conformational analysis is carried out using molecular dynamics methods. In this modeling process, both protein and the complexed ligand are allowed to sample different 3D conformational states until the most favorable state is reached or found to exist between protein and inhibitor. The final structure as proposed by

the molecular dynamics analysis is analyzed visually to make sure the modeled complex is in accord with known experimental SAR based on measured binding affinities.

References

- 5    (1) Magnuson, K., *et al.*, *Microbiological Reviews*, 57:522-542 (1993).
- (2) Lynen, F., *Eur. J. Biochem.*, 112:431-442 (1980).
- (3) Wakil, S. J., *et al.*, *Annu. Rev. Biochem.*, 52:537-579 (1983).
- (4) B. Shen, B., *et al.*, *J. Bacteriol.*, 174:3818 (1992).
- (5) Hopwood, D. A., and Sherman, D. H., *Annu. Rev. Genet.*, 24:37-66 (1990).
- 10    (6) Kleinkauf, H., and Von Dohren, H., *Eur. J. Biochem.*, 236:335-351 (1996).
- (7) Marahiel, M. A., *FEBS Lett.*, 307:40 (1992).
- (8) White, R. H., *Biochemistry*, 19:9-15 (1980).
- (9) Sanyal, I., *et al.*, *Am. Chem. Soc.*, 116:2637-2638 (1994).
- (10) Rawlings, M. and J.E.J. Cronan, *FASEB J.*, 2:A1559 (1988).
- 15    (11) Hill, R.B., *et al.*, *Protein Expression and Purification*, 6:394-400 (1995).
- (12) Rock, C.O. and J.E.J. Cronan, *Anal. Biochem.*, 102:362-364 (1980).
- (13) Holak, T.A., *et al.*, *Eur. J. Biochem.*, 175:9-15 (1988).
- (14) Furukawa, H., *et al.*, *J. Bacteriol.*, 175:3723-3729 (1993).
- (15) Bergler, H., *et al.*, *J. Biol. Chem.*, 269, 5493-5496 (1994).
- 20    (16) Banerjee, A., *et al.*, *Science*, 263:227-230 (1994).
- (17) Dessen, A., *et al.*, *Science*, 267:1638-1641 (1995).
- (18) Quémard, A., *et al.*, *Biochemistry*, 34:8235-8241 (1995).
- (19) Lambalot, R. H., *et al.*, *Chemistry & Biology*, 3:923-936 (1996).
- (20) Elovson, J. and Vagelos, P. R., *J. Biol. Chem.*, 243:3603 (1968).
- 25    (21) Lambalot, R. H. and Walsh, C. T., *J. Biol. Chem.*, 270:24658-24661 (1995).
- (22) Reuter, K., *et al.*, *The EMBO Journal*, 18:6823-6831 (1999).
- (23) Otwinowski, Z. and W. Minor, *Methods Enzymol.*, 276:307-326 (1997).
- (24) Navaza, J., *Acta Crystallogr.*, A50:157-163 (1994).

- (25) Brunger, A.T., *et al.*, *Acta Crystallographica*, D54:905-921 (1998).
- (26) Lambalot, R. H., and Walsh, C.T., *J. Biol. Chem.*, 270: 24658-61 (1995).
- (27) Fischl, A.S., and Kennedy, E.P., *J. Bacteriol.*, 172: 5445-9 (1990).
- (28) Kay, L.E., *Prog. Biophys. Molec. Biol.*, 63: 110-126 (1995).
- 5 (29) Delaglio, F., *et al.*, *J. Biomol. NMR*, 6: 277-293 (1995).
- (30) Zhu, G., and Bax, A., *J. Magn. Reson.*, 100: 202-7 (1992).
- (31) Garrett, D. S., *et al.*, *J. Magn. Reson.*, 95: 214-20 (1991).
- (32) Muhandiram, D. R., and Kay, L. E., *J. Magn. Reson., Ser. B*, 103: 203-16 (1994).
- 10 (33) Grzesiek, S., *et al.*, *J. Biomol. Nmr*, 3: 487-93 (1993).
- (34) Bax, A., Max, D., and Zax, D., *J. Am. Chem. Soc.*, 114: 6923-5 (1992).
- (35) Bax, A., *et al.*, *J. Biomol. Nmr*, 4: 787-97 (1994).
- (36) Pascal, S. M., *et al.*, *J. Magn. Reson., Ser. B*, 103: 197-201 (1994).
- (37) Marion, D., *et al.*, *Biochemistry*, 28: 6150-6 (1989).
- 15 (38) Zuiderweg, E. R. P., and Fesik, S. W., *Biochemistry*, 28: 2387-91 (1989).
- (39) Cornilescu, G., *et al.*, *J. Biomol. NMR*, 13: 289-302 (1999).
- (40) Wuthrich, K., *et al.*, *J. Mol. Biol.*, 169: 949-961(1983).
- (41) Clore, G. M., *et al.*, *Biochemistry*, 26: 8012-23 (1987).
- (42) Wagner, G., *et al.*, *J. Mol. Biol.*, 196: 611-39 (1987).
- 20 (43) Nilges, M., *et al.*, *Protein Eng*, 2: 27-38 (1988).
- (44) Clore, G. M., *et al.*, *Biochemistry*, 29: 1689-96 (1990).
- (45) Brunger, A. T. *X-PLOR Version 3.1 Manual*, Yale University, New Haven, CT (1993).
- (46) Kuszewski, J., *et al.*, *J. Magn. Reson., Ser. B*, 106: 92-6 (1995).
- 25 (47) Kuszewski, J., *et al.*, *Protein Sci.*, 5: 1067-1080 (1996).
- (48) Kuszewski, J., *et al.*, *J. Magn. Reson.*, 125: 171-177 (1997).
- (49) Laskowski, R. A., *et al.*, *J. Appl. Cryst.* 26, 283-291 (1993).
- (50) Laskowski, R., *et al.*, *Biomol NMR*, 8: 477-486 (1996).
- (51) Wakil, S. J., *et al.*, *Annu. Rev. Biochem*, 52: 537-79 (1983).

- (52) Majerus, P. W., and Vagelos, P. R., *Advan. Lipid Res*, 5: 1-33 (1967).
- (53) Prescott, D. J., and Vagelos, P. R., *Advan. Enzymol. Relat. Areas Mol. Biol*, 36: 269-311 (1972).
- (54) Shen, B., et al., *J. Bacteriol.*, 174: 3818-21 (1992).
- 5 (55) Baldwin, J. E., et al., *J. Antibiot.*, 44: 241-8 (1991).
- (56) Rusnak, F., et al., *Biochemistry*, 30: 2916-27 (1991).
- (57) Geiger, O., et al., *J. Bacteriol.*, 173: 2872-8 (1991).
- (58) Issartel, J. P., et al., *Nature*, 351: 759-61 (1991).
- (59) Takiff, H. E., et al., *J. Bacteriol.* 174: 1544-53 (1992).
- 10 (60) Lambalot, R. H., and Walsh, C. T., *J. Biol. Chem.*, 270: 24658-61 (1995).
- (61) Crump, M. P., et al., *Biochemistry*, 36: 6000-6008 (1997).
- (62) Holak, T. A., et al., *Biochemistry*, 27: 6135-42 (1988).
- (63) Holak, T. A., et al., *FEBS Lett.*, 242: 218-24 (1989).
- (64) Clore, G. M., and Gronenborn, A. M., *Protein Science*, 3: 372-390 (1994).
- 15 (65) Arrowsmith, C. H., and Wu, Y.-S., *Prog. Nucl. Magn. Reson. Spectrosc.*, 32: 277-286 (1998).
- (66) Clore, G. M., and Gronenborn, A. M., *Trends Biotechnol.*, 16: 22-34 (1998).
- (67) Clore, G. M., et al., *J. Mol. Biol.*, 231: 82-102 (1993).
- (68) Ghose, R., et al., *FEBS Lett.*, 388: 66-72 (1996).
- 20 (69) Oswood, M. C., et al., *Proteins: Struct., Funct., Genet.*, 27: 131-143 (1997).
- (70) Grzesiek, S., and Bax, A., *J. Am. Chem. Soc*, 114: 6291-3 (1992).
- (71) Grzesiek, S., et al., *J. Magn. Reson., Ser. B*, 101: 114-19 (1993).
- (72) Vuister, G. W., and Bax, A., *J. Am. Chem. Soc*, 115: 7772-7 (1993).
- (73) Kay, L. E., et al., *J. Magn. Reson.*, 89: 496-514 (1990).
- 25 (74) Petros, A. M., et al., *FEBS Lett.*, 308: 309-14 (1992).
- (75) Gemmecker, G., et al., *J. Magn. Reson.*, 96: 199-204 (1992).
- (76) Ikura, M., and Bax, A., *J. Am. Chem. Soc.*, 114: 2433-40 (1992).
- (77) Archer, S. J., et al., *J. Magn. Reson.*, 95: 636-41 (1991).

- (78) Bax, A., and Pochapsky, S. S., *Journal of Magnetic Resonance*, 99: 638-643 (1992).
- (79) Powers, R., *et al.*, *J. Magn. Reson.*, 94: 209-13 (1991).
- (80) Vuister, G. W., *et al.*, *J. Am. Chem. Soc*, 114: 9674-5 (1992).
- 5 (81) Grzesiek, S., *et al.*, *J. Am. Chem. Soc*, 117: 5312-15 (1995).
- (82) Zuiderweg, E. R. P., *et al.*, *J. Magn. Reson*, 86: 210-16 (1990).
- (83) Ikura, M., *et al.*, *J. Magn. Reson*, 86: 204-9 (1990).
- (84) Lee, W., *et al.*, *FEBS Lett.*, 350: 87-90 (1994).
- (85) Clore, G. M., *et al.*, *Biochemistry*, 29: 5671-6 (1990).
- 10 (86) Kleywelt, G. J., and Jones, T. A., *Methods Enzymol.*, 277: 208-230 (1997).

All publications mentioned herein above, whether to issued patents, pending applications, published articles, or otherwise, are hereby incorporated by reference in their entirety. While the foregoing invention has been described in some detail for purposes of clarity and understanding, it will be appreciated by one skilled in  
15 the art from a reading of the disclosure that various changes in form and detail can be made without departing from the true scope of the invention in the appended claims.